RSC Advances

ROYAL SOCIETY OF CHEMISTRY

www.rsc.org/advances

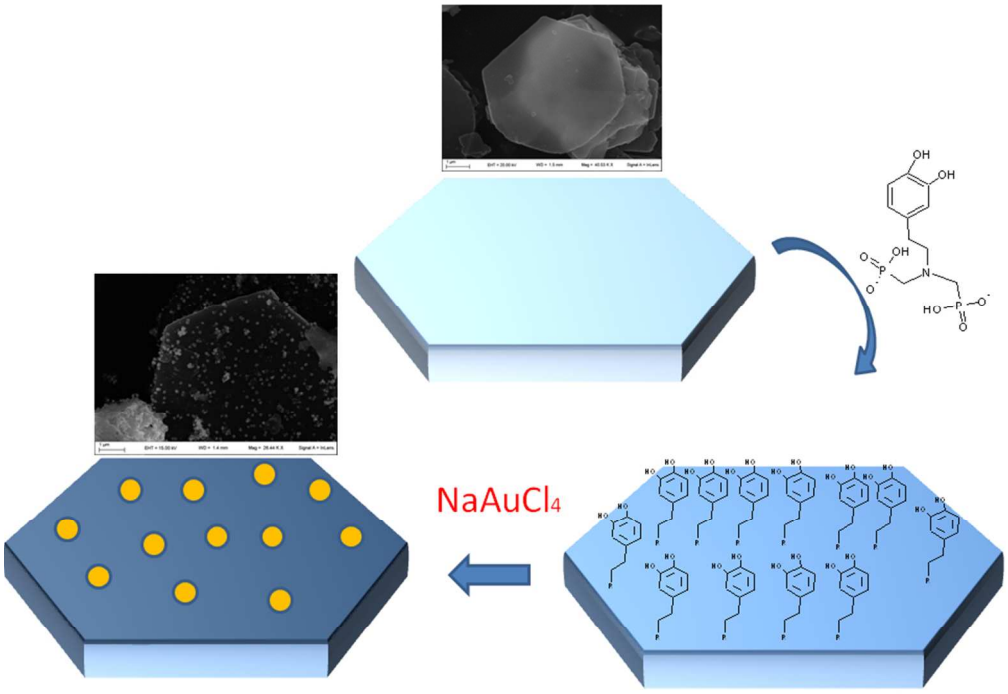

254x190mm (96 x 96 DPI)

Journal Name

RSCPublishing

PAPER

Redox Properties of LDH Microcrystals Coated with a Catechol-bearing Phosphonate derived from Dopamine.

Cite this: DOI: 10.1039/x0xx00000x

Received 00th January 2012,
Accepted 00th January 2012

DOI: 10.1039/x0xx00000x

www.rsc.org/

Maria de Victoria Rodríguez,[a] Ernesto Brunet[a], Morena Nocchetti[b], Federica Presciutti[c] and Ferdinando Costantino*[c,d]

The surface of Zn-Al-chloride LDH microcrystals (LDH = Layered Double Hydroxides) was activated by grafting a redox active catechol bearing bis-phosphonate obtained by dopamine derivatization. The obtained phosphonate uniformly coats the LDH crystals surface and the catechol groups are exposed. The redox activity of the catechol was employed for the quick and easy synthesis of Gold NPs, which are supported onto the LDH microcrystal surface. The synthetic procedures and the complete characterization of the hybrid system is reported.

Introduction

Catechol bearing molecules can be found in a very high number of natural and biological processes, including neurosignalling,[1] photoprotection,[2] metal complexation,[3] and surface adhesion.[4]

The latter characteristic is typical of dopamine (3,4-dihydroxyphenylalanine) which is responsible of the mussel foot protein adhesion. This feature has been recently employed as bio-mimetic tool for the design of highly adhesive mussel inspired films and materials, thanks to the facile polymerization of dopamine into polydopamine. The catechol-redox activity of the dopamine was also recently used to induce the reduction of noble metals into metal nanoparticles (NPs) giving rise to several hybrid systems, based on polydopamine polymer and noble metal NPs.[5] Among them we can cite the synthesis of adhesive mussel-inspired films containing Au and Ag NPs with high conductive properties,[6] with antimicrobial activity[7] and core-shell system for imaging and antitumoral activity.[8]

Actually, one of the major challenges of this chemistry is focused on the coupling of such active hybrid systems with other materials which can act both as solid support and that could embody an added value due to their intrinsic properties (such as TiO_2, graphene, carbon nanotubes and so on). Among 2D materials, layered double hydroxides (LDHs) epitomize one of the most prevalent compounds actually used for a huge number of applications such as catalyst in many processes,[9] controlled drug delivery systems,[10] gas capture,[11] water purifier[12] or in biomedical applications.[13]

Herein we report on the surface modification of well crystallized ZnAl-LDH microcrystals achieved by grafting it with a catechol-bearing phosphonate derived from dopamine, in order to impart redox properties to the system. The redox properties of this new hybrid system were then employed for the synthesis of gold nanoparticles (AuNPs) stabilized onto the LDH surface through the oxidation to quinone of the catechol groups exposed on the surface.

Experimental

Instrumental details

PXRD patterns for Rietveld refinements were collected with Cu Kα radiation on a PANalytical X'PERT PRO diffractometer, PW3050 goniometer equipped with an X'Celerator detector. The long fine focus (LFF) ceramic tube operated at 40 kV and 40 mA. To minimize preferential orientations of the microcrystals, the samples were carefully side-loaded onto an aluminum sample holder with an oriented quartz monocrystal underneath. Thermogravimetric (TG) measurements were performed using a Netzsch STA490C thermoanalyser under a 20 mL min^{-1} air flux with a heating rate of 5 °C min^{-1}. FE-SEM images were collected with a LEO 1525 ZEISS instrument working with an acceleration voltage of 15 kV. TEM images were collected with Philips 208 Transmission Electron Microscope (TEM). A small drop of the dispersion was deposited on a copper grid that had been pre-coated with a Formvar film and then evaporated in air at RT. UV-Vis spectrometry was performed by using a Deuterium-Halogen lamp as excitation source, (emitted light from 200 to 1100 nm) and a high sensitive CCD spectrometer (Avaspec 2048 USB2, 200-1100 nm range, spectral resolution 8 nm). Three single 400 micron core fibres direct the light from the source to the analysing surface. ^{1}H and ^{13}C spectra were recorded on Bruker AV-300 (300MHz, 75.5 MHz respectively), ^{31}P and ^{19}F-NMR spectra were recorded on Bruker AVII-300 (121 MHz and 282 MHz respectively) in the indicated solvents. Transmittance mid-FT-IR measurements were carried out with a JASCO FT / IR 4000

spectrophotometer. The spectral range collected was 400 to 4000 cm^{-1}, with a spectral resolution of 2 cm^{-1} acquiring 100 scans. The samples were dispersed on anhydrous KBr pellets. Metal and phosphorus analyses were performed with Varian 700-ES series inductively coupled plasma-optical emission spectrometers (ICP-OES). A weighted amount of the samples (about 10 mg) was dissolved in concentrate HCl/HNO_3 3/1 v/v and the solution was brought to a final volume of 50 ml. The solution properly diluted was analyzed by ICP. Elemental analysis were also performed on a LECO CHNS-932 analyzer in the SIdI, UAM. Total Reflection X-Ray Fluorescence (TXRF) measurements were performed on a 8030C Atomika spectrometer using a direct solid method. The spectrometer is equipped with a X-Ray tube of 3kW and a multilayer monocromator. The measurements were performed using 50kV, 8500cps of speed and time acquisition of 500s. The microwave equipment was a Biotage initiator 2.5.

Syntheses

Synthesis of $H_4P_2O_6$DOPA

[{[2-(3,4-dihydroxyphenyl)ethyl]imino}di(methylene)]bis(phosphonic acid), hereafter $H_4P_2O_6$DOPA, was prepared by a modified Mannich type reaction[14] starting from a doubly protected dopamine. The procedure involved the protection of both catechol and the amino groups in order to prevent polymerization of the dopamine and the formation of π-conjugated complexes like quinidrone.

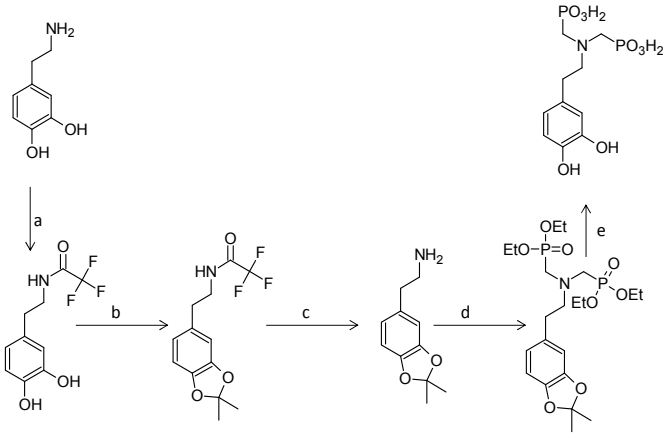

Scheme 1. Synthetic procedure to prepare $H_4P_2O_6$DOPA. Reagents, conditions and yields: (a) CF_3COOMe, Et_3N in MeOH, 12h r.t., 86%; (b) 2,2-dimethoxypropane, p-TsOH in Benzene, 4h reflux, 90%; (c) $LiOH{\cdot}H_2O$ in THF/H_2O 4h r.t., 87%; (d) HCOH, Diethylphosphite, 2h 120°C, 55%; (e) HCl 37% 12h reflux, 100%.

One of the main problems of catechol is its quick oxidation to the quinone form. Due to this, the key step in the synthesis of the $H_4P_2O_6$DOPA is the protection of this group in order to avoid oxidation. In the presence of an amino group direct protection of a catechol group, by acetonide formation is not possible due to the high reactivity of the amino group thus forcing its protection first. The procedure of this initial stage was performed at room temperature by treating dopamine hydrochloride with methyl trifluoroacetate in methanol in the presence of triethylamine.[15] This protection would be easily removed as shown later on in the scheme. Then, the catechol group was protected building the aforementioned acetonide in high yield by refluxing trifluoracetate-dopamine with 2,2-dimethoxypropane (DMP) in the presence of a catalytic amount of *p*-toluenesulfonic acid (*p*-TsOH). In order to shift the equilibrium reaction, the water formed was removed with a soxhlet extractor filled with $CaCl_2$ or activated molecular sieves. Once the catechol is protected, the next step is the introduction of the anchoring phosphonic groups so that the amino protection needs to be removed, maintaining catechol's. Once more, this reaction was performed at room temperature under very mild conditions using LiOH in a H_2O/THF solution. Then the diphosphonate anchoring group can be introduced. However, conventional Irani synthesis cannot be directly carried out by using formaldehyde and H_3PO_3 because, in those strong acidic conditions, deprotection of catechol and its polymerization readily occurs. Therefore, a modified Irani reaction has been performed by refluxing acetonide-protected dopamine in the presence of paraformaldehyde and diethylphosphite.[16] The last stage in the synthesis of $H_4P_2O_6$DOPA is the hydrolysis of phosphonate groups and deprotection of catechol that was performed on a single step by refluxing in concentrated HCl. The detailed procedure is reported in ESI.

Synthesis of ZnAl-Chloride LDH

Crystalline ZnAl-Chloride LDH (ZnAl-Cl) was synthesized by modifying the "Urea-method".[17] $ZnCl_2$ (13.637 g, 100 mmol), $AlCl_3{\cdot}6H_2O$ (10.505 g, 43.5 mmol) and urea (10.44 g, 173.82 mmol) were refluxed in 300 mL of deionized water for 24 h. The precipitate was centrifuged and washed three times with deionized water. The Zn/Al molar ratio was evaluated by means of ICP analysis and the water content was evaluated by thermogravimetric analysis yielding the following formula $[Zn_{0.67}Al_{0.33}(OH)_2]Cl_{0.33}{\cdot}0.6H_2O$.

Synthesis of ZnAl/$H_2P_2O_6$DOPA

In a microwave tube ZnAl-Cl (750 mg) was dispersed in 6.5 mL of H_2O. Dopamine (417 mg, 1.22 mmol) was dissolved into a solution of 1 mL of KOH 2M and added to LDH-Cl. The mixture was then heated at 120ºC for 45 minutes under nitrogen using normal absorption into a Biotage initiator 2.5 microwave oven. The resulting solid was centrifuged, washed twice with deionized water and dried at 50ºC for 6h.

Synthesis of Au@ZnAl/$H_2P_2O_6$DOPA

8 mL of a solution of $NaAuCl_4$ in water (0.0125 M, 4.5 mg/mL) was added slowly to a suspension of 100 mg of LDH containing dopamine in 10 mL of CO_2-free deionizated water. The reaction mixture turned into dark red color and was stirred for 12 h at r.t. under nitrogen and protected from light. The resulting solid was centrifuged, washed twice with deionizated water and dried at 50ºC for 6 h.

Results and Discussion

The surface of ZnAl-Cl was functionalized by using microwaves with anions of $H_4P_2O_6$DOPA obtained by partial deprotonation of the phosphonic group in 2M KOH. A 2:1 molar ratio of KOH/ $H_4P_2O_6$DOPA (4 acid protons/mol of phosphonic acid) was used with the aim of obtain $H_2P_2O_6DOPA^{2-}$ di-anion in which two acid protons are maintained.

The $H_2P_2O_6DOPA^{2-}$ anions exchange the Cl^- anions of the LDH and, upon dehydration at 50°C, a grafting reaction between the acid P-OH and the OH- groups of the lamella occurs. The appearance of a small absorption band around 1000 cm^{-1} can be ascribed to fully

deprotonation of P-OH groups and the formation of M-O-P bonds (see Fig. 1S, ESI).[18] The loss of one water molecule per phosphonic group also occurred. The diffraction pattern of ZnAl/$H_2P_2O_6$DOPA (Figure 2) is typical of the ZnAl-Cl, having an interlayer distance of 7.75 Å, indicating that the exchange reaction of $H_2P_2O_6$DOPA involved only the LDH surface and that did not occur into the interlayer region of the LDH.

Figure 1 schematizes the exchange/grafting reaction of the $H_2P_2O_6$DOPA anions onto the surface of hexagonal ZnAl-Cl microcrystals. The content of Zn, Al, P, N, O, C and H in ZnAl/$H_2P_2O_6$DOPA was determined by ICP, CHN elemental analysis and TXRF, considering a quantitative grafting reaction the composition resulted $[Zn_{0.67}Al_{0.33}(OH)_{1.896}]Cl_{0.226}(P_2O_6DOPA)_{0.052}\cdot 0.23H_2O$. Analysis calculated C : H : N for ZnAl/$H_2P_2O_6$DOPA was 6.01 : 2.92 : 0.70 and found 5.96 : 3.11 : 0.71.

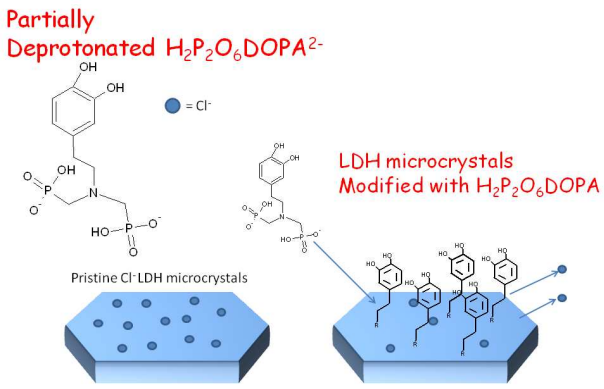

Figure 1 Schematic representation of the exchange/grafting reaction of $H_2P_2O_6$DOPA anions onto the LDH surface.

A $NaAuCl_4$ aqueous solution was added to a ZnAl/$H_2P_2O_6$DOPA aqueous dispersion, the mixture turned into dark red color indicating that the Au(III) ions were quickly reduced to gold nanoparticles on the LDH surface by the catechol groups. X-ray diffraction pattern of the recovered composite Au@LDH/$H_2P_2O_6$DOPA shows (Figure 2) the reflections of cubic gold beside the ZnAl-Cl reflections.

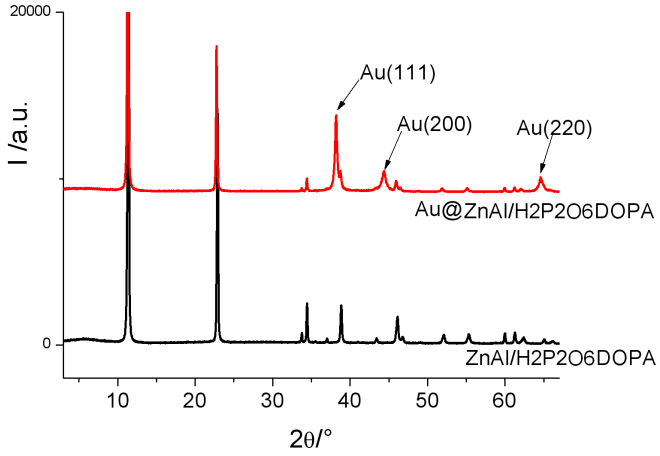

Figure 2 XRPD patterns of the **ZnAl/$H_2P_2O_6$DOPA** and of **Au@ZnAl/$H_2P_2O_6$DOPA** LDH

Rietveld refinement of the Au@ZnAl/$H_2P_2O_6$DOPA diffraction pattern allowed to get information on the volume weighted crystalline domain size of Au nanoparticles and on the relative quantitative phase analysis of the two components.

Microstructural analysis was performed by using the GSAS program.[19] Table 1S reports the instrumental and refinement details. First, the instrumental contribution to the peak broadening was previously evaluated by the Rietveld refinement of the profile of lanthanum hexaboride (LaB_6), as an external peak profile standard. We assumed that the standard was not affected by microstrain, and the instrumental broadening was modeled by the refinement of W and Y peak shape parameters for Gaussian and Lorentzian contributions, respectively. Coherent domain size (volume weighted) parallel ($D\|$) and perpendicular ($D\perp$) to the (200) and to the (111) directions was calculated by using the following expressions

$$D\| = 1800\lambda/\pi(X + Xe) \text{ and } D\perp = 1800\lambda/\pi X$$

Microstrain as source of peak broadening was also considered. In order to give an average strain value along the selected direction a simple strain model (%) was also used by refining the Gaussian and the Lorentzian contribution Y, Ye and Yi where Yi is the experimental instrumental contribution obtained with the LaB_6 standard. The equation for the strain % $\varepsilon\|$ and $\varepsilon\perp$ to the selected broadening axes are

$$\varepsilon\| = (\pi/18000)(Y + Ye - Yi) \text{ and } \varepsilon\perp = (\pi/18000)(Y - Yi)$$

Where λ is the wavelength and X and Xe are two terms related to the Lorentzian contribution of the size broadening effect.

The calculation gave as results an average $D\|200$crystalline domain size of about 16 nm whereas the $D^{\perp}200$ is about 100 nm.

The $D\|111$ and $D^{\perp}111$ were 34 and 12 nm respectively. These data roughly indicate the crystalline domain sizes measured along and perpendicular to the selected directions and generally they do not correspond to the observed size from electron microscope images. In our case a size anisotropy perpendicular to the (200) seems to be present. Concerning the microstrain the only predominant effect, nicely related to the peak broadening effect, can be detected only on the direction perpendicular to (200) which is $\varepsilon\perp$ ($x10^3$) = 1.9. The calculation carried out on different directions did not give any valuable result. This means that, along that direction, strain efficiently contributes to the broadening. The high D value found for that plane (200) is then affected by the strain contribution and it is probably overestimated. Quantitative phase analysis was carried out by using the Bish and Howard formula.[20]

$$Wm = \frac{a_m S_m}{\sum_{k=1}^{k=m} a_k S_k}$$

where Wm and a_k are the weighed fraction of the m^{th} component in the sample and its calculated density, respectively; a_k is given as follows: $a_k = Z_k M_k U_k$ where Z_k, M_k, and U_k are the number of chemical formula units in a unit cell, the molecular weight, and the unit-cell volume, respectively. The calculation, in absence of amorphous phases, gave as result 22% of Au.

Assuming that the only amorphous contribution to the mixture can be ascribed to the presence of the $H_2P_2O_6$DOPA anions coating (calculated on the basis of the molar fraction =

18.5 wt %), the normalized relative phase weight percentages were LDH = 64.9%, Au = 16.6%.

The value calculated from quantitative analysis is 0.138 mol of Au/mol of Au@LDH/ $H_2P_2O_6$DOPA that is in good agreement with the value found by elemental analysis (ICP and TXRF) (0.127 mol of Au/ mol of compound). The elemental analysis of Au@ZnAl/$H_2P_2O_6$DOPA showed that the content of Zn and Al was different from the ZnAl/$H_2P_2O_6$DOPA starting material. In particular after Au deposition the solid was enriched in Al. The oxidation of catechol groups to quinone groups occurs with the formation of H^+ ions that locally decrease the pH.[21] LDHs at low pH value can undergo to a partial dissolution with a preferential leaching of the more soluble cation that is Zn. This process on the one hand leads to a partial dissolution of LDH on the other hand drives the catechol oxidation reaction to right promotion the formation of metallic gold clusters. Considering that the maximum aluminium molar fraction possible for LDH is 0.40 a segregation of $Al(OH)_3$ was hypothesized and the composition of the solid was then written as $[Zn_{0.60}Al_{0.40}(OH)_{1.834}]Cl_{0.234}(P_2O_6DOPA)_{0.083}Au_{0.127}0.3H_2O$ + 0.04 $Al(OH)_3$. Analysis calculated for Au@ZnAl/$H_2P_2O_6$DOPA C : H : N was 6.59 : 2.41 : 0.77 and found 6.38 : 2.77 : 0.77.

Rietveld plot is shown in Figure 3 whereas the complete refinement parameters and procedures are reported in ESI, table 1S.

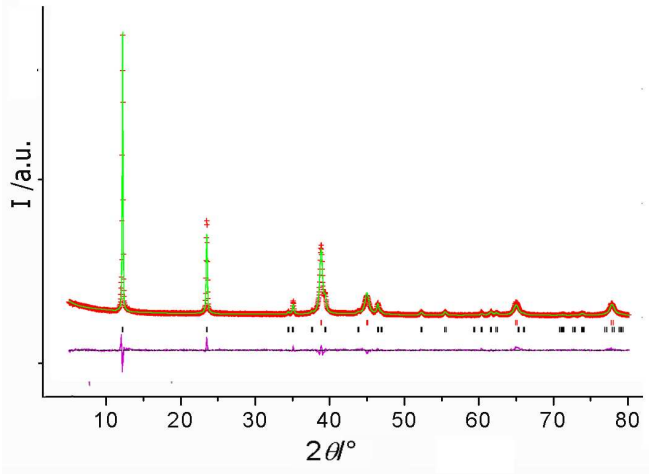

Figure 3 Rietveld plot of **Au@ZnAl/$H_2P_2O_6$DOPA^{2-}**LDH

FE-SEM and TEM images of the pristine LDH and of the Au@LDH/$H_2P_2O_6$DOPA microcrystals are shown in figure 4.

Figure 4a (FE-SEM) shows the pristine ZnAl-LDH microcrystals; it should be remarked that the surface of the crystals was well polished. After the modification with $H_2P_2O_6$DOPA anions the crystal surface turned into dark colour and, at higher magnification degree (figures 4c and 4d) it also became corrugated. Indeed, small globular structures of size < than 10 nm were homogeneously present over the entire surface. These structures cannot be attributed to smaller gold clusters as they are not present in the equivalent TEM images which are more sensitive to the atomic weight (figures 4e and 4f).

This also suggests that the modification of the LDH microcrystals with $H_2P_2O_6$DOPA anions occurred efficiently with a homogeneous covering of the surface with the organic molecules.

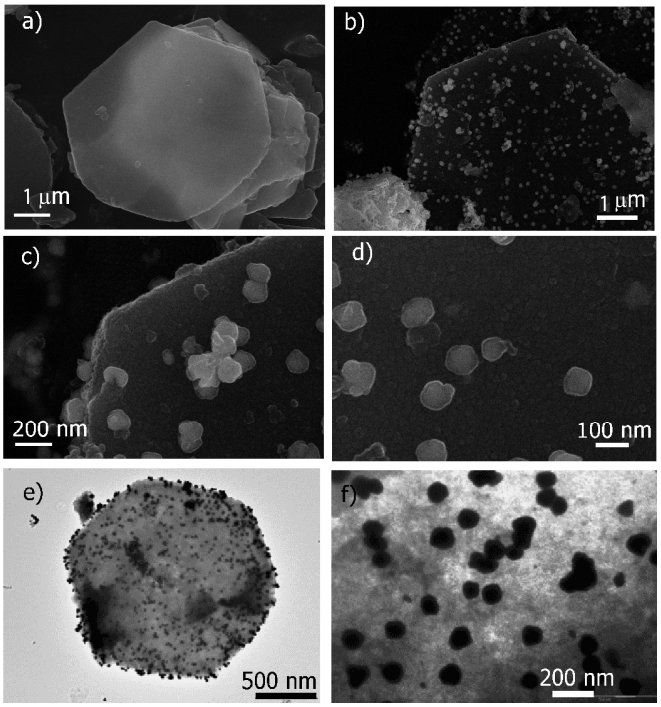

Figure 4 FE-SEM (a-d) and TEM (e-f) images of pristine (a), and modified (b-f) ZnAl-LDH microcrystals.

Gold NPs are well dispersed over the entire LDH crystal surface and they look to apparently bear spherical shape with a narrow size distribution ranging from 60 to 90 nm. Some of them are aggregated in larger clusters formed by 4 or 5 NPs each.

Surface Plasmonic Resonance (SPR) spectra were also collected on the bulk solid. The absorption spectrum is reported in Figure 5.

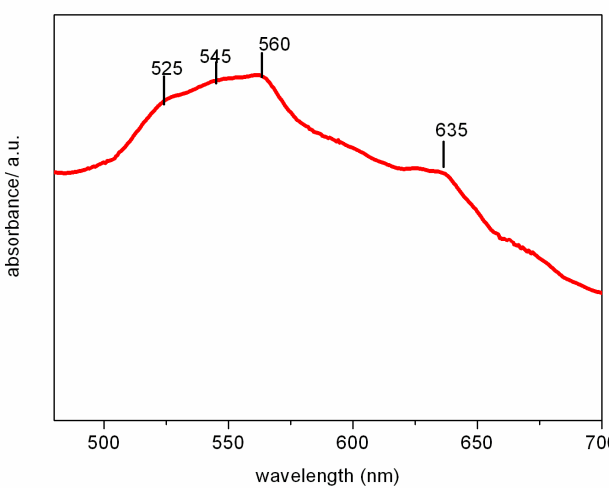

Figure 5 Uv-vis spectrum of Au@ZnAl/$H_2P_2O_6$DOPA. The SPR signals at 525, 545 and 560 nm are indicated.

SPR spectrum shows three distinct peaks (determined by second derivative of the curve) at 525, 545 and 560 nm. This confirms the polydisperse nature of the gold nanoclusters.

According to El-sayed and Link[22] the position of the SPR signals can be related with the average particle size for monodisperse systems. In our case the predominant 560 nm signal is indicative of 70 to 90 nm size gold clusters. The signals at 545 and 525 nm can be related to 50 and 25 nm clusters size respectively. A fourth signal around 635 nm can be ascribed to one of the absorption modes of quinone or metal coordinated hydro-quinones.[23]

These data are in good agreement with the FE-SEM and TEM images. LDH as solid supports for AuNPs have been recently reported from other authors and these materials were mainly employed for catalytic purposes.[24]

The NPs were grown on the LDH crystal surface by using conventional reduction methods involving citrate or urea as precipitating agent. The average size of AuNPs reported in other papers was generally lower than that reported in our work (5 to 20 nm, *vs* 40 to 90 nm). Nevertheless, respect to the conventional methods, the catechol coating LDHs appear to be more efficient in terms of Au(0) conversion, allowing the precipitation of higher amount of Au, expressed as weight %.

Moreover, found density of Au NPs onto the LDH crystal surface by us was generally higher than that reported in other papers. The effort to improve the tuning the size/shape of the gold cluster, by changing the initial amount of Au and other parameters like solvents and temperature, will be carried out in the near future.

Conclusions

In this paper the organic synthesis of a catechol-bearing phosphonic acid, derived from dopamine, has been reported. With respect to dopamine, the reactivity of this novel phosphonate is drastically changed due to the non availability of the $–NH_2$ which precludes the possibility of self-polymerization into polydopamine.

The $H_2P_2O_6$DOPA anions have been then used to uniformly coat the surface of well crystallized LDH hexagonal crystals, the exposed catechol groups operating as the redox agent for the stabilization of polydisperse gold NPs. Respect to the conventional methods, this strategy is "template free" and allows to increase the absolute amount of gold nanoclusters onto the LDH surface. However, the disadvantage of this system resides in the scarce control of the gold NPs size and shape. We plan to address further applications of the catechol-bearing LDH in different fields, like the grafting of magnetic NPs and the complexation of catalytic metals and/or luminescent lanthanide ions for advanced applications in heterogenous catalysis, theranostic and imaging.

Acknowledgements

F.C. and M. N. thank Project FIRB 2010 No. RBFR10CWDA_003 for the financial support.

Notes and references

[a]*Departamento de Química Orgánica, Facultad de Ciencias, Universidad Autónoma de Madrid, 28049 Madrid, Spain.*

[b]*Dipartimento di Scienze Farmaceutiche, University of Perugia, Via del Liceo 1, 06123, Perugia, Italy.*

[c]*Dipartimento di Chimica, Biologia e Biotecnologie, University of Perugia, Via Elce di Sotto 8, 06123, Perugia, Italy.*

[d] *CNR – ICCOM, Via Madonna del Piano 10, 50019, Sesto Fiorentino, Firenze, Italy. Email: ferdinando.costantino@unipg.it*

† Footnotes should appear here. These might include comments relevant to but not central to the matter under discussion, limited experimental and spectral data, and crystallographic data.

Electronic Supplementary Information (ESI) available: [complete synthetic procedures, Rietveld refinement details, FT-IR spectra]. See DOI: 10.1039/c000000x/

1. *(a)* S. Callier, M. Snapyan,S. L. Crom, D.Prou, J.-D. Vincent and P.Vernier, *Biol. Cell.,* 2003, **95**, 489–502; *(b)* A. Zhang, J. L. Neumeyer and R. J. Baldessarini, *Chem. Rev*., 2007, **107**, 274–302.

2. M. Brenner and V. Hearing, *J. Photochem. Photobiol.*, 2008, **84**, 539 – 549.

3. *(a)* K. G. Alley, G. Poneti, P S. D. Robinson, A. Nafady, B. Moubaraki, J. B. Aitken, S. C. Drew, C. Ritchie, B. F. Abrahams, R. K. Hocking, K. S. Murray, A. M. Bond, H. H. Harris, L. Sorace and C. Boskovic, *J. Am. Chem. Soc.*, 2013, **135**, 8304–8323; *(b)* A. Dei, G. Poneti and L. Sorace *Inorg. Chem.*, 2010, **49**, 3271–3277.

4. *(a)* J. H. Waite, *Int. J. Adhes. Adhes*. 1987, **7**, 9–14; *(b)* J. H. Waite, *Integr. Comp. Biol*., 2002, **42**, 1172–1180.

5. *(a)* H. Hartati, M. Santoso, S. Triwahyono and D. Prasetyoko, *Bulletin of Chemical Reaction Engineering and Catalysis,* 2013, **8**, 14-33; *(b)* I. Reyero, G. Arzamendi and L.M.Gandía, *Key Engineering Materials*, 2013, **571**, 1-26.

6. *(a)* Y. Long, J. Wu, H. Wang, X. Zhang, N. Zhao and J. Xu, *J. Mater. Chem*., 2011, **21**, 4875-4881; *(b)* G. J Gou, L. E. Dong, F. J. Bao, Z. Y. Wang, L. Jiao, J. Huang, Y. Sun and B. Bing Xue, *Applied Mechanics and Materials*, 2013, **320**, 495-504.

7. D. E. Fullenkamp, J. G. Rivera, Y- Gong, K. H. A. Lau, L. He, R. Varshney and P. B. Messersmith, *Biomaterials,* 2012, **33**, 3783-3791.

8. Y. Lee, H. Lee, Y. Beom Kim, J. Kim, T. Hyeon, H. Wook Park, P. B. Messersmith and T. G. Park, *Adv. Mater*., 2008, **20**, 4154–4157

9. *(a)* A. Vaccari, *Appl. Clay Sci.*, 1999, **14**, 161-168; *(b)* M. Turco, G. Bagnasco, U. Costantino, F. Marmottini, T. Montanari, G. Ramis and G. Busca, *J. Catal.,* 2004, **228**, 43-55; *(c)* T. Montanari, M. Sisani, M. Nocchetti, R. Vivani, M. Concepcion Herrera Delgado, G. Ramis, G. Busca and U. Costantino, *Catal. Today,* 2010, **152**, 104- 109; *(d)* G. Busca, U. Costantino, T. Montanari, G. Ramis, C. Resini and M. Sisani, *Int. J. Hydrogen Energy,* 2010, **35**, 5356-5366; *(e)* A. Fronzo, C. Pirola, A. Comazzi, C. L. Bianchi, A. Di Michele, R. Vivani, M. Nocchetti, M. Bastianini, D. C. Boffito and F. Galli, *Fuel*, 2014, **119**, 62–69; *(f)* I. Reyero, G. Arzamendi and L. M. Gandía, *Key Engineering Materials*, 2013, **571**, 1-26.

10. *(a) Clays and Health Clays* in *Pharmacy, Cosmetics, Pelotherapy, and Environmental Protection,* Special Issue of *Appl. Clay Sci.* ed. M I. Carretero and G. Lagaly, 2007, vol. 36; *(b)* V. Ambrogi, V. Ciarnelli, M. Nocchetti, L. Perioli and C. Rossi, *Eur. J. Pharm. Sci.* 2009, **73**, 285–291; *(c) LDH in physical, chemical, bio-chemical and life sciences* in *Developments in Clay Science* – Volume 5B Handbook of Clay Science: Techniques and Applications, ed. F. Bergaya and G. Lagaly, 2013, vol. 5B; *(d)* L. Li, W. Gu, J. Chen, W. Chen and Z. P. Xu, *Biomaterials,* 2014, **35**, 3331-3339; *(e)* V. Rives, M. del Arco and C. Martín, *Appl. Clay Sci.*, 2014, **88-89**, 239-269.

11. *(a)* H. H. Q. Wang, Z. Tay, J. Zhong, Luo and A. Borgna, *Energy Environ. Sci*., 2012, **5**, 7526-7530; *(b)* O. Aschenbrennera, P. McGuireb, S. Alsamaq, J. Wang, S. Supasitmongkola, B. Al-Durib, P. Styringa and J. Wood, *Chem. Engin. Res. and Des*., 2011, **89**, 1711–1721

12. F. L. Theiss, S .J. Couperthwaite, G. A. Ayoko and R. L. Frost, *J. of Colloid and Interface Science,* 2014, **417**, 356.

13. *(a)* U. Costantino, V. Ambrogi, L. Perioli and M. Nocchetti, *Micropor. Mesopor. Mater.*, 2008, **107**, 149-160; *(b)* J.-M. Oh, S.-J. Choi, G.-E. Lee, S.-H. Han and J.-H. Choy, *Adv. Funct. Mater.*, 2009, **19**, 1617-1624; *(c)* E. Ruiz-Hitzky, P. Aranda, M. Darder and G. Rytwo, *J. Mater. Chem.*, 2010, **20**, 9306-9321; *(e)* L. Perioli, V. Ambrogi, M. Nocchetti, M. Sisani and C. Pagano, *Appl. Clay Sci.*, 2011, **53**, 696-703; *(f)* U. Costantino, F. Costantino, F. Elisei, L. Latterini and M. Nocchetti, *PCCP*, 2013, **15**, 13254-13269; *(g)*

M. Nocchetti, A. Donnadio, V. Ambrogi, P. Andreani, M. Bastianini, D. Pietrella and L. Latterini, *J. Mater. Chem. B,* 2013, **1**, 2383–2393.
14. K. Moedritzer and R. R. Irani, *J. Org. Chem*., 1966, **31**, 1603-1606.
15. Z. Liu, B. Hu and P. B. Messersmith, *Tetrahedron Letters*, 2010, **51**, 2403.
16. A. A. Prishchenko, M. V. Livantsov, O. P. Novikova, L. I. Livantsova and V. S. Petrosyan, *Heteroatom Chemistry*, 2010, **21**, 430-440.
17. *(a)* U. Costantino, F. Marmottini, M. Nocchetti and R. Vivani, *Eur. J. Inorg. Chem.*, 1998, **10**, 1439-1446. *(b)* M. Bastianini, D. Costenaro, C. Bisio, L. Marchese, U. Costantino, R. Vivani, M. Nocchetti, *Inorg. Chem.,* 2012*,* **51***,* 2560.
18. *(a)* U. Costantino, M. Casciola, L. Massinelli, M. Nocchetti and R. Vivani, *Solid State Ionics*, 1997, **97**, 203-212; *(b)* U. Costantino, S. Clementi, M. Nocchetti and R. Vivani, *Mol. Cryst. Liquid Cryst.*, 1998, **311**, 207- 210.
19. C. Larson, R. B. von Dreele, Generalized Crystal Structure Analysis System; Los Alamos National Laboratory: Los Alamos, NM, 2001.
20. D. L. Bish and S. A. Howard, *J. Appl. Crystallogr*., 1998, **21**, 86-91.
21. Sirajuddin, A. Mechler, A. A. J. Torriero, A. Nafady, C. Y. Lee, A. M. Bond, A. P. O'Mullane and S. K. Bhargava, *Colloid Surface A*, 2010, **370**, 35-41.
22. S. Link and M. A. El-Sayed, *J. Phys. Chem. B*, 1999**, 103***,* 4212-4217.
23. M. J. Sever and J. J. Wilker, *Dalton Trans* 2004, 1061-1072
24. *(a)* J. Zhao, X. Kong, W. Shi, M. Shao, J. Han, M. Wei, D. G. Evans and X. Duan, *J. Mater. Chem.*, 2011, **21**, 13926-13933; *(b)* F. Zhang, X. Zhao, C. Feng, B. Li, T. Chen, W. Lu, X. Lei and S. Xu, *ACS Catal.*, 2011, **1**, 232–237; *(c)* Y. Wang, D. Zhang, M. Tang, S. Xu and M. Li, *Electrochimica Acta*, 2010, **55**, 4045–4049.

